ORIGINAL PAPER

First principles calculations of the electronic and chemical properties of graphene, graphane, and graphene oxide

**J. J. Hernández Rosas · R. E. Ramírez Gutiérrez ·
A. Escobedo-Morales · Ernesto Chigo Anota**

Abstract The electrical and chemical properties of graphene ($C_{24}H_{12}$), graphane ($C_{24}H_{24}$) and graphene oxide ($C_{54}H_{17}+O+(OH)_3+COOH$) were studied through the density functional theory (DFT) at level of Local Density Approximation (LDA) using a model C_nH_m like. The optimized geometry, energy gap and chemical reactivity for the proposed carbon 2D models are reported. It was found that while the graphene and graphane structures have semiconductor behavior, the graphene oxide behaves as semi-metal. However, a transition from semi-mental to semiconductor is predicted if the carboxyl group (COOH) is removed from such structure. The chemically active sites are analyzed on the basis of the electrophilic Fukui functions for each structure.

Keywords Density functional theory · Graphane ·
Graphene · Graphene oxide

Introduction

Since the experimental isolation of graphene in 2004 [1], and a single sheet of boron nitride by Geim et al. [2], one year later, the interest in two dimensional (2D) nano-

J. J. Hernández Rosas · A. Escobedo-Morales ·
E. Chigo Anota (✉)
Facultad de Ingeniería Química,
Benemérita Universidad Autónoma de Puebla,
C.P. 72570 Puebla, Pue., Mexico
e-mail: echigoa@yahoo.es

R. E. Ramírez Gutiérrez
Facultad de Ciencias Químicas,
Benemérita Universidad Autónoma de Puebla,
C.P. 72570 Puebla, Pue., Mexico

structures increased noticeably. The 2D nanostructures have been identified as potential building blocks for gas sensors [3], high density data storage devices [4], and nanoelectronics [5, 6]. Graphene is among the most promising nanomaterials for structural applications due to its novel mechanical properties [7]. This 2D nanostructure can be stabilized through hydrogenation process, and the experimental results reveal that it behaves as a wide band gap semiconductor, as was predicted by Sofo et al. in 2007 [8, 9]. Another interesting geometrical conformation of carbon sheets is the graphane, which unlike graphene shows non-planar topography. Elias et al. [10] reported the first experimental evidence of graphane structure using scanning and transmition electron microscopies, demonstrating that controlling the chemical characteristics of graphane is feasible to bring the graphene structure back.

Recently, Dikin et al. [11] have reported experiments concerning chemical modification of graphene. They incorporated oxygen atoms, hydroxyl and carboxylic acid groups in the structure of graphene to obtain the so-called graphene oxide, material with interesting mechanical properties like its large bulk modulus.

In the field of theoretical calculations, several C_nH_m-like structures have been explored by Chigo [12] to study 2D carbon structures, and doping process of graphene and boron nitride sheets with nitrogen and carbon atoms. On the other hand, similar structures have been used successfully in theoretical studies of F and Li doping of boron nitride sheets [13], physical properties of boron nitride oxide structure [14], electronic properties of III-A nitrides [15], and adsorption of water in 2D boron nitride [16]. However, the study of structural and electronic properties of 2D nanostructures remains as a challenge for theoretical scientist. The understanding of the physical properties of

such structures is a main feature for their successful application in nanoelectronic devices.

Here, we present a theoretical study of the electronic and chemical properties of graphene ($C_{24}H_{12}$), graphane coronene ($C_{24}H_{24}$), and graphene oxide ($C_{55}H_{17}+O+(OH)_3+COOH$) models applying the density functional theory (DFT) at the level of local density approximation (LDA); furthermore, a study of the effect of the incorporation of hydroxyl and carboxyl groups on the electronic properties of the graphene oxide structure is presented. Figure 1 shows the schematic representation of the 2D structures used in this study.

Computational methodology

Geometrical optimization and electronic properties

Briefly, the molecular calculations were performed using the DMOL^3 code [17] based in the DFT [18–20] at the level of LDA. We apply the Perdew-Wang extended hybrid functional (PWC) [21] for the correlation-exchange term and the double numeric polarized atomic base (DNP) [17, 22, 23] at the level of all electrons in singlet state and null charge for the treatment of the core. The cut of the orbital was at 0.3 nm, with tolerance of 1.0×10^{-6} Ha for the self consistent field cycle (SCF). Optimal structural geometry, dipolar moment and electronic gap energy (arithmetic difference between the energies of the HOMO and LUMO) were calculated at standard conditions of temperature and pressure. Non-negative vibrational frequencies were used as stability criterion for the obtained structures [24]. In order to validate the simulated models, the cohesion energy of naphthalene ($C_{10}H_8$), phirene ($C_{16}H_{10}$), coronene ($C_{24}H_{12}$), and the cluster $C_{55}H_{18}$ were calculated, obtaining the value of 3.82 a.u./atom for all of the systems.

Chemical properties

In order to elucidate the chemical reactivity of the simulated models the Fukui functions corresponding to each structure was obtained. It was calculated using the correlation-exchange hybrid functional B3LYP [25–27], included in the GAUSSIAN03 code [28], and the base function of divided valence 6-31+G(d,p) [29] visualized throughout the gOpenmol software [30].

Results and discussion

Graphene and graphane models

Figures 2a and b show the structures for graphene and graphane models, respectively. It can be seen that while graphene sheet remains as a flat surface, graphane shows a perceptible deviation respect to a flat structure, instead a coronene armchair structure is obtained. Such structural conformation of graphane was previously used by Martínez et al. [31] and experimentally demonstrated by You et al. [32] using Raman spectroscopy, showing that it is possible to determine the chirality of carbon sheets through this optical technique.

Table 1 summarizes the structural parameters and magnitudes of dipolar moment of the optimized models. It can be noted that the bond lengths of C-C and C-H of graphene and graphane differ slightly, 0.099 and 0.005 Å, respectively; furthermore, unlike graphene structure, the carbon polygons seem distorted in the graphane model.

According to our DFT calculations, both of the structures, graphene and graphane, behave as a semiconductor material, with gap energies of 2.95 and 3.87 eV, respectively. Lebegue et al. [33] report gap energies of 5.4 and 4.9 eV for armchair and boat configuration of graphane, respectively. Nevertheless, it is important to
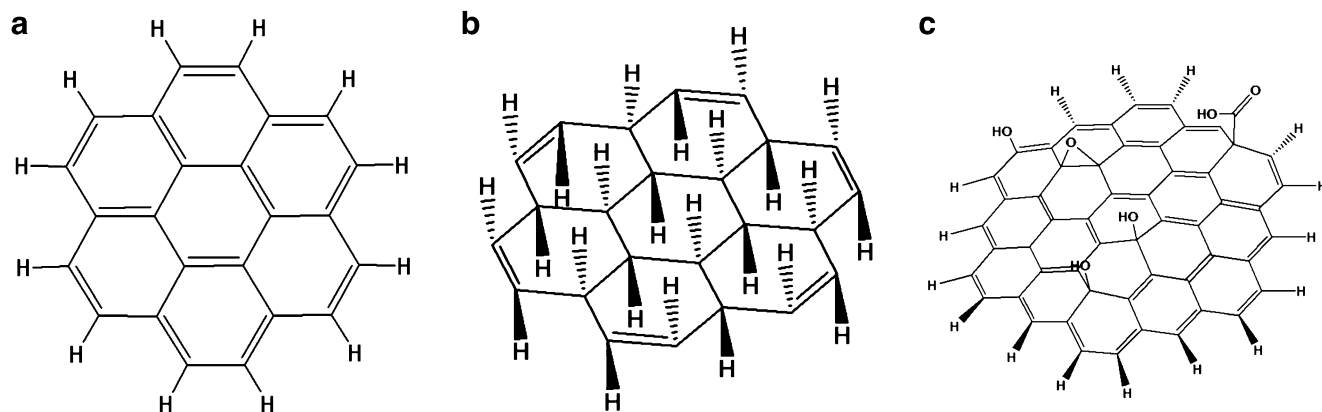

Fig. 1 Schematic representation of (a) graphene, (b) graphane, and (c) graphene oxide structures
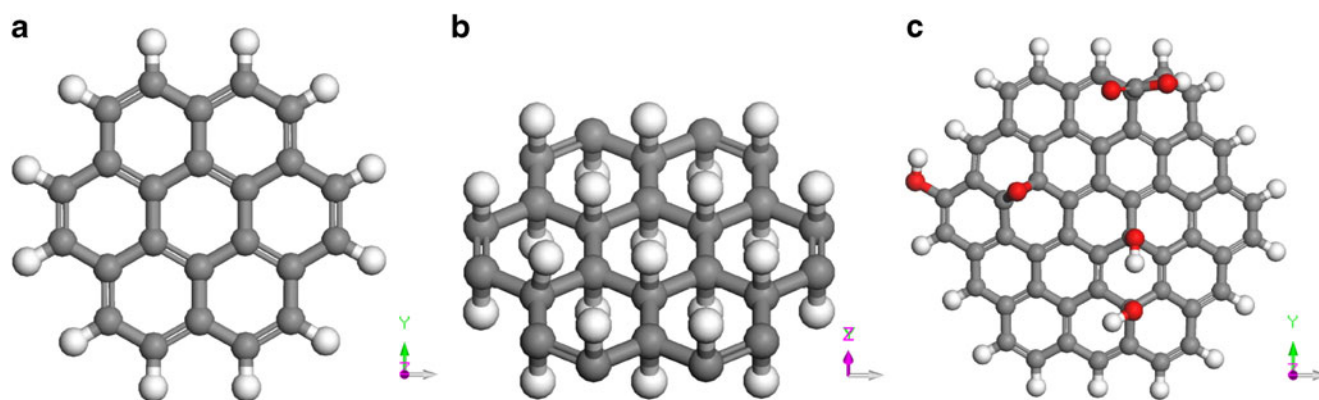
Fig. 2 Initial models for (**a**) graphene ($C_{24}H_{12}$), (**b**) graphane ($C_{24}H_{24}$), and (**c**) graphene oxide ($C_{55}H_{17}+O+(OH)_3+COOH$)

point out that those energies were estimated using a solid treatment.

Graphene oxide model

Figure 2c shows the model for graphene oxide. The circular geometry of the studied carbon structures was chosen in order to avoid anisotropic effects that may be introduced due to differences of the size of the modeled structure on considering a specific direction. In favor of the proposed model, it is worth noting that such symmetry has been successfully used to study physical properties of 2D carbon and boron nitride sheets [12, 15, 34, 35], suggesting that it could be applied for graphene oxide.

From Fig. 2c, it can be seen that the incorporation of hydroxyl and carboxyl groups trends to bend slightly the structure of graphene, resulting in a curved surface.

The calculated gap energy for graphene oxide was 0.42 eV, and therefore a semi-metal behavior is recognized.

Larger values for the gap energy of graphene oxide can be found in the literature, with either low oxidation (1.4 eV) or high oxidation states (3.2 eV) [36].

The graphene oxide has larger polar character than graphene and graphane structures, as indicates the magnitudes of their dipolar moment (Table 1). However, the polarity of graphene is considerably lower than that of boron nitride (15.85 Debye) [14].
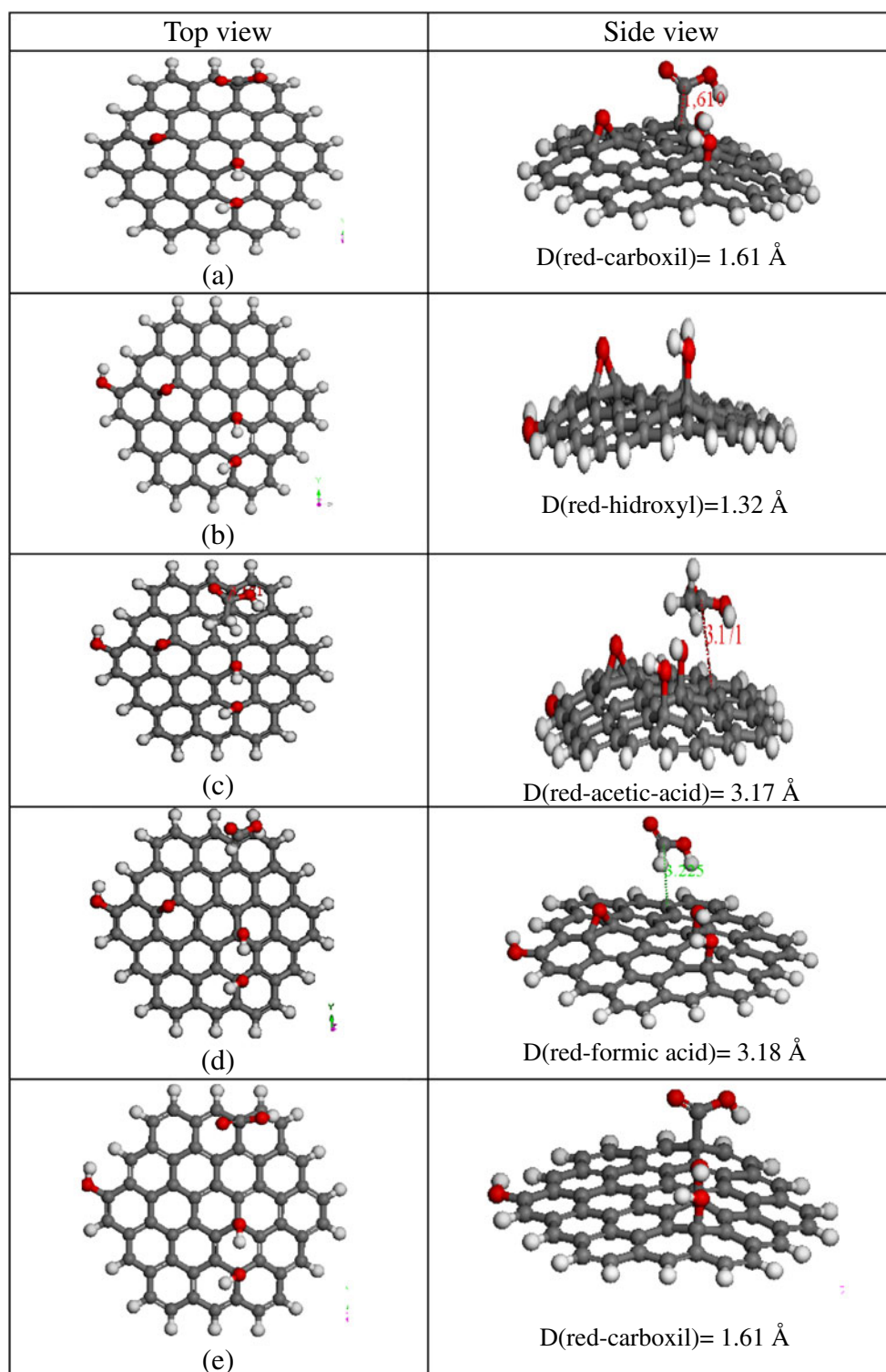
In order to study the influence of the hydroxyl and carboxyl groups on the electronic properties of graphene oxide, we calculated the gap energies of several structures with and without those radical groups. Figure 3 shows the optimized geometries for the different modeled structures. It was found that on removing the carboxyl group the gap energy increases up to 1.134 eV (see Table 2) suggesting a semimetal-semiconductor transition; on the other hand, on releasing the hydroxyl groups form the surface of graphene oxide it decreases even further (0.404 eV). It is worth noting that on removing the carboxyl group the magnitude

Table 1 Structural parameters and magnitudes of dipolar moment of the optimized graphene, graphane, and graphene oxide models

System	Bond length (Å)			Bond angle C-C-C (degrees)	Dipolar moment (Debye, $\times 10^{-3}$)
	C-C	C-H	O-H		
Graphene ($C_{24}H_{12}$)	1.411	1.095		119.95	2.3
Graphene ($C_{55}H_{18}$)	1.410	1.096		120.4	17
Graphane ($C_{24}H_{24}$)	1.51	1.1		110-122	3.4
	1.52†				
	1.56‡				
Graphene oxide	1.41	1.095	0.97	120.1	6470
Graphene oxide with two OH groups	1.41	1.094	0.99	120.1	6750
Graphene oxide without carboxyl group	1.41	1.095	0.982	120.2	2821
Graphene oxide with CH_3COOH group*	1.41	1.094	0.983	120.1	4593
Formic acid					3790
Acetic acid					1740

† Armchair conformation [8]; ‡ boat conformation [8]; * unstable

Fig. 3 Optimized models (**a**) graphene oxide with 2 OH, (**b**) without carboxyl group, (**c**) with acetic acid, (**d**) with formic acid, (**e**) with oxygen

Top view	Side view
(a)	D(red-carboxil)= 1.61 Å
(b)	D(red-hidroxyl)=1.32 Å
(c)	D(red-acetic-acid)= 3.17 Å
(d)	D(red-formic acid)= 3.18 Å
(e)	D(red-carboxil)= 1.61 Å

of the dipolar moment decreases considerably, even below that calculated for formic acid (see Table 1), suggesting that the carboxyl group is responsible of the polarity of graphene oxide.

The structure of graphene oxide becomes unstable when the carboxyl group (COOH) was interchanged by either acid formic (HCOOH) or acetic acid (CH$_3$COOH). Furthermore, those functional groups depart from the surface

Table 2 Summary of the calculated energy gaps of the studied systems and its comparison with those results found in the literature

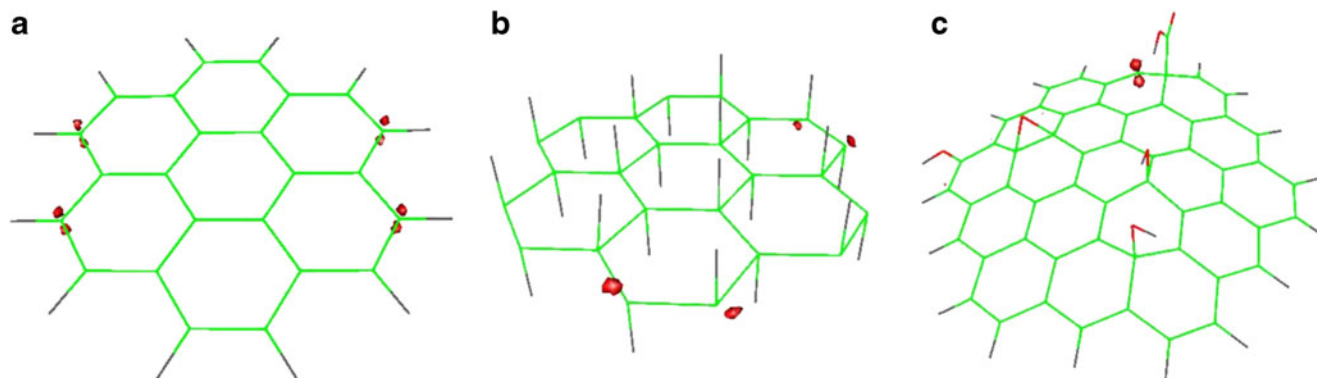| System	Gap energy (eV)	Reference
Graphene ($C_{24}H_{12}$)	2.95[a]	This work
	2.8[b]	[31]
	2.7[a]	[31]
Graphene ($C_{55}H_{18}$)	1.94[a]	This work
Graphane ($C_{24}H_{24}$)	3.87[a]	This work
	5.97[c]	[47]
	5.4[c]	[33]
	3.42[a]	[47]
Graphene oxide ($C_{55}H_{17}+O+(OH)_3+COOH$)	0.42[a]	This work
Graphene oxide without COOH group	1.134[a]	This work
Graphene oxide with CH_3COOH group*	1.96[a]	This work
Graphene oxide with HCOOH group*	1.14[a]	This work
Graphene oxide with two OH groups	0.404[a]	This work
Graphite oxide (low oxidation)	1.4	[36]
Graphite oxide (high oxidation)	3.2	[36]

[a] LDA; [b] GGA; [c] GW; * unstable

by 3.184 and 3.17 Å, respectively. The same effect was obtained when the oxygen atom of the epoxy group was removed from the 2D structure.

Chemical reactivity

From the viewpoint of hard and soft acids and bases (HSAB) [37, 38] the electrophilic and nucleophilic character of a molecular system can be elucidated calculating the Fukui function [39]. This function represents the change of the electronic density $\rho(r)$ with respect to the number of electrons N, i.e., $f(r) = (\partial \rho(r)/\partial N)_{v(r)}$; it can be evaluated for electrophilic, nucleophilic, and radical attacks, namely $f^-(r)$, $f^+(r)$, $f^{\,o}(r)$ Fukui functions, respectively [40–43]. The interpretation of the Fukui function is based on the principle that the regions of a system where such function is large are chemically softer than the regions where it is small; therefore it is possible to establish the chemical behavior of localized sites for an specific system [44].

Figure 4 shows the calculated electrophilic Fukui functions of graphene, graphane, and graphene oxide models. According to the calculated Fukui functions for graphene (Fig. 4a), four regions susceptible to electrophilic attack were recognized. These regions are located on the periphery of the structure, just above carbon atoms. It is worth noting that the spatial distribution of these sites do not reflect the hexagonal symmetry of the system. No region susceptible to electrophilic attacks located at the C-C bounds of the hexagonal sub-lattices was identified.

Politzer, et al. [45] have shown that sites most vulnerable to electrophilic attacks of a molecular system can be found through the calculation of the average local ionization energy on the molecular surface, $\bar{I}s(r)$; here the locations of the lowest values of such function, $\bar{I}s,\min(r)$, correspond with the least tightly-held electrons, and therefore, the most reactive sites. In this sense the $f^-(r)$ and $\bar{I}s(r)$ functions can be directly co-related; however, analogous arguments do not apply for the $f^+(r)$ Fukui function.

Fig. 4 Electrophilic Fukui function of (**a**) graphene (isosurface: 0.01 u.a.), (**b**) graphane (isosurface: 0.025 u.a.), and (**c**) graphene oxide models (isosurface: 0.01 u.a.)

The average local ionization energy computed by Peralta et al. [46] for several graphene systems suggests that the most susceptible regions for electrophilic interactions are localized on the periphery ($C_{62}H_{20}$), in agreement with our results; however, it is worth to point out that, they are distributed around all the periphery of the graphene system as is expected.

The calculated $f^-(r)$ Fukui function for graphane structure is shown in Fig. 4b. Like in the graphene model, the most susceptible regions for electrophilic attacks are distributed on the periphery; however they are not localized above carbon atoms, instead such regions approach to C-C bound midpoints, may be due to the double-bound character of these sites.

Finally, the Fukui function $f^-(r)$ calculated for graphene oxide structure (Fig. 4c) shows a region susceptible to electrophilic attacks near the carboxyl group. It may be due to the increase of the electronic density at specific points as a result of chemical functionalization. No similar effect was observed at the central portion of the carbon sheet where the oxygen and hydroxyl groups were chemisorbed; the last can be attributed to the nearly radial distribution of chemical hardness of the carbon structure [46] and differences among the electronegativity of the chemisorbed species.

Conclusions

The optimized structural parameters of the graphene and graphane models obtained through the density functional theory are in agreement with the data previously reported; similar coincidence are observed for the gap energy calculated for these 2D carbon systems. It is proposed that these models can be used to calculate other physical properties, like ionicity. While graphene and graphane structures have small dipolar moment, the graphene oxide structure shows strong polar character; such behavior can be attributed to the adsorption of chemical groups, mainly COOH.

The obtained results suggest that it is feasible to control the electronic properties of graphene oxide through a careful selection of the chemical radicals adsorbed on its surface. Whereas on removing a hydroxyl group a decrease of the gap energy is observed, the release of the carboxyl group results in a semimetal-semiconductor transition.

The analysis of graphene, graphene oxide and graphane structures with the electrophilic Fukui function show preferential chemical reactivity on the periphery of the system, this is valid for all the modeled structures.

Finally, it was found that the descriptions provided by the DFT at the level of LDA of the electronic and chemical properties of the studied 2D models are in good agreement with previous studies based in a solid treatment; suggesting that a cluster model can provide a reasonable description of the structural, electronic and chemical properties of larger 2D nanostructures.

References

1. Novoselov KS, Geim AK, Morozov SV, Jiang D, Zhang Y, Dubonos SV, Grigorieva IV, Firsov AA (2004) Science 306:666–669
2. Novoselov KS, Jiang D, Schedin F, Booth TJ, Khotkevich VV, Morozov SV, Geim AK (2005) Proc Natl Acad Sci USA 102:10451–10453
3. Schedin F, Geim AK, Morozov SV, Hill EW, Blake P, Katsnelson MI, Novoselov KS (2007) Nat Mater 6:652–655
4. Serrano J, Bosak A, Arenal R, Krisch M, Watanabe K, Taniguchi T, Kanda H, Rubio A, Wirtz L (2007) Phys Rev Lett 98:095503–095504
5. Bolotin KI, Sikes KJ, Hone J, Strormer HL, Kim P (2008) Phys Rev Lett 101:096802–096804
6. Bolotin KI, Sikes KJ, Jiang Z, Klima M, Fudenberg G, Hone J, Kim P, Stormer HL (2008) Solid State Commun 146:351–355
7. Leenaerts O, Partoens B, Peeters FM. arXiv:0810.4056v1 [cond-mat.mtrl-sci]
8. Sofo JO, Chaudhari AS, Barber GD (2007) Phys Rev B 75:153401–153404
9. Boukhvalov DW, Katsnelson MI, Lichtenstein AI (2008) Phys Rev B 77:035427
10. Elias DC, Nair RR, Mohiuddin TMG, Morozov SV, Blake P, Halsall MP, Ferrari AC, Boukhvalov DW, Katsnelson MI, Geim AK, Novoselov KS (2006) Science 323:610–613
11. Dikin DA, Stankovich S, Zimney EJ, Piner RD, Dommett GHB, Evmenenko G, Nguyen ST, Ruoff RS (2007) Nature 448:457–460
12. Chigo-Anota E (2009) Sup y Vac 22:19–23
13. Chigo-Anota E, Salazar-Villanueva M, Hernández-Cocoletzi H. Phys Stat Solidi C in press. doi:10.1002/pssc.200983909
14. Chigo-Anota E, Salazar-Villanueva M, Hernández-Cocoletzi H. J Nanosci Nanotechnol in press. doi:10.1166/jnn.2011.3441
15. Chigo-Anota E, Salazar-Villanueva M, Hernández-Cocoletzi H (2010) Phys Stat Solidi C 7:2252–2254
16. Chigo-Anota E, Salazar-Villanueva M (2009) Sup y Vac 22:23–28
17. Delley B (1990) J Chem Phys 92:508–517
18. Kohn W, Becke AD, Parr RG (2006) J Phys Chem 100:12974–12980
19. Jones RO, Gunnarsson O (1989) Rev Mod Phys 61:689–746
20. Kohn W (1999) Rev Mod Phys 71:1253–1266
21. Perdew JP, Wang Y (1992) Phys Rev B 45:13244–13249
22. Delley B (1996) J Phys Chem 100:6107–6110
23. Delley B (2000) J Chem Phys 113:7756–7764
24. Foresman JB, Frisch Æ (1996) Exploring chemistry with electronic structure methods, 2nd edn. Gaussian Inc, USA, p 300
25. Becke AD (1993) J Chem Phys 98:5648–5652
26. Lee C, Yang W, Parr RG (1988) Phys Rev B 37:785–789
27. Stephens PJ, Devlin FJ, Chabalowski CF, Frisch MJ (1994) J Phys Chem 98:11623–11627
28. Frisch MJ et al. (2004) GAUSSIAN03, revision C.02. Gaussian Inc, Wallingford

29. Szabo A, Ostlund NS (1989) Modern quantum chemistry: introduction to advanced electronic structure theory. Mc Millan, USA, p 480
30. http://www.csc.fi/english/pages/g0penMol. Consulted online June 2010
31. Martínez JI, Cabria I, López MJ, Alonso JA (2009) J Phys Chem C 113:939–941
32. You YM, Ni Zh H, Yu T, Shen ZX (2008) Appl Phys Lett 93:163112–163113
33. Lebegue S, Klintenberg M, Eriksson O, Katsnelson MI. arXiv:0903.0310v1 [cond-mat.mtrl-sci]
34. Gómez-Navarro C, Thomas Weitz R, Bittner AM, Scolari M, Burghard M, Kern K (2007) Nano Lett 7:3499–3503
35. Sun X, Liu Z, Welsher K, Robinson JT, Goodwin A, Zaric S, Dai H (2008) Nano Res 1:203–212
36. Lahaye RJWE, Jeong HK, Park CY, Lee YH (2009) Phys Rev B 79:125435–125438
37. Pearson RG (1963) J Am Chem Soc 85:3533–3539
38. Gázquez JL, Méndez F (1994) J Phys Chem 98:4591–4593
39. Parr RG, Yang W (1984) J Am Chem Soc 106:4049–4050
40. Méndez F, Gázquez JL (1994) J Am Chem Soc 116:9298–9301
41. López P, Méndez F (2004) Org Lett 6:1781–1783
42. Parr RG, Yang W (1989) Density functional theory of atoms and molecules. Oxford University Press, USA, p 342
43. Lee Ch, Yang W, Parr RG (1988) J Mol Struct THEOCHEM 163:305–313
44. Gilardoni F, Weber J, Chermette H, Ward TR (1998) J Phys Chem A 102:3607–3613
45. Politzer P, Murray JS, Burat FA (2010) J Mol Model in press. doi: 10.1007/s00894-010-0709-5
46. Peralta-Inga Z, Murray JS, Grice ME, Boyd S, O'Connor CJ, Politzer P (2001) J Mol Struct THEOCHEM 549:147–158
47. Sahin H, Ataca C, Ciraci S (2009) Appl Phys Lett 95:222510–222513